J. Fluid Mech. (1987), *vol.* 180, *pp.* 515–527
Printed in Great Britain

A study of peristaltic flow

By C. POZRIKIDIS
Research Laboratories, Eastman Kodak Company Rochester, NY 14650, USA

(Received 25 September 1986)

Peristaltic flow in two-dimensional channels with sinusoidal waves is analysed. Under the assumption of creeping motion, the problem is formulated using the boundary integral method for Stokes flow. The effect of channel width, wave amplitude, phase shift, and mean pressure gradient on the streamline pattern and the properties of the flow is considered. The results are discussed with reference to various physiological and engineering processes. It is suggested that under the quasi-steady approximation, peristaltic flow with a varying mean pressure gradient offers an efficient method for molecular–convective transport.

1. Introduction

Peristaltic flows are generated by the propagation of waves along the flexible walls of a channel. These flows provide an efficient means for sanitary fluid transport and thus, they are exploited in industrial peristaltic pumping. In physiological and medical applications, peristaltic flows are used for the transport of blood within small blood vessels or artificial blood devices.

Two interesting phenomena associated with peristaltic flows are fluid trapping and material reflux. The former describes the development and downstream transport of free eddies, called fluid boluses. The latter refers to the net upstream convection of fluid particles against the travelling boundary waves. These two phenomena are of great physiological significance, as they may be responsible for thrombus formation in blood, and pathological transport of bacteria. From the standpoint of fluid mechanics, these phenomena demonstrate the complexity, but also motivate the fundamental study of peristaltic flows.

Taylor (1951) studied peristaltic flows with reference to swimming of microscopic organisms. Subsequent studies were motivated by interest in physiological fluid transport, and the realization that peristaltic pumping may be used for the efficient transport of slurries, and sensitive or corrosive fluids. Jaffrin & Shapiro (1971) reviewed early work including experimental observations and asymptotic solutions. In the following years many studies appeared analysing among other topics particle transport in peristaltic flows (Hung & Brown 1976), effect of peripheral layers (Shukla, Parihar & Rao 1980), and effect of non-Newtonian characteristics, (Bohme & Friedrich 1983). A few numerical studies have also been presented. Tong & Vawter (1972) used a finite element method to conduct a preliminary study in the limit of creeping motion. Brown & Hung (1977) used a finite difference scheme based on curvilinear coordinates, and concentrated on the effects of inertia and on the mechanical energy transfer characteristics. Takabatake & Ayukawa (1982) presented finite different solutions at moderate Reynolds numbers, and demonstrated the limitations of previous asymptotic expansions. It is clear that the absence of an efficient numerical method has prohibited an extended analysis for general flow conditions.

In this paper we consider peristaltic flow in two-dimensional channels under the assumption of creeping motion. Addressing this basic assumption of our analysis, we note that although the absence of inertia may depend on the particular application, it constitutes an accurate approximation for many physiological processes (Jaffrin & Shapiro 1971). For instance, Shapiro, Jaffrin & Weinberg (1969) as well as Lykoodis & Roos (1970) estimate the Reynolds number of peristaltic flow in the human ureter to be of the order of unity, demonstrating the insignificance of inertial forces. The goal of our analysis is then to describe the structure and properties of the flow as a function of geometrical channel characteristics and flow conditions. The use of the boundary integral method for Stokes flow constitutes an essential part of our analysis by allowing a detailed, accurate, and relatively extensive investigation. Our calculations complement previous efforts and reveal certain novel flow phenomena.

In §2 we formulate the problem and discuss the method of solution. In §3 we study pure peristaltic flow, and in §4 we consider the interaction between peristaltic and pressure driven motion. We conclude in §5 by briefly discussing peristaltic flow with asymmetric waves.

2. Formulation of the problem

We consider periodic flow in a two-dimensional channel with oscillating walls, under conditions of creeping motion. For extensible walls with sinusoidal peristaltic waves, we assume that the y-position of fluid particles on the upper and lower wall is given by

$$\left.\begin{aligned} y_1 &= w+a_1 \cos(k(x-ct)-2\phi), \\ y_2 &= -w-a_2 \cos(k(x-ct)), \end{aligned}\right\} \qquad (1)$$

respectively, while their x-position remains constant (figure 1). In the above equations k is the wavenumber, c is the wave speed, and ϕ is the phase difference between the two walls, $0 < \phi < \frac{1}{2}\pi$. The case $\phi = 0$ corresponds to symmetric waves, whereas the case $\phi = \frac{1}{2}\pi$ corresponds to asymmetric, bending waves (Wilson & Panton 1979). Since in a frame of reference moving at the wave speed c the flow is steady, it is convenient to introduce the new coordinate $z = x-ct$, and to consider the flow in the (z, y)-plane.

In general, the flow may be driven by two independent mechanisms: the peristaltic motion and the presence of a mean pressure gradient $G = -\mathrm{d}P/\mathrm{d}x$. The relative strength of these two components may be expressed by the parameter $K = Gw^2/\mu c$. Under the above definitions, we study the flow as a function of K, the geometrical parameters w/λ, a_1/λ, a_2/λ, and the phase shift ϕ.

At low Reynolds numbers, $Re = cw^2/\nu\lambda$, the flow is governed by the Stokes equation and hence, the problem may be formulated using the boundary integral method for Stokes flow. For details on the mathematical formulation, notation, and the numerical method, see Pozrikidis 1987 §§2 and 3. Here we briefly mention that the method requires the discretization of one period of the upper or lower wall in a number of straight segments, and the local approximation of the force as a constant function, and of the velocity as a linear function over each segment. Given the boundary velocity, the boundary force is evaluated using a collocation method which reduces the problem to the solution of a system of linear algebraic equations. The choice of fundamental solution required in the above procedure is dictated by the wave characteristics. For $a_1 = a_2$ the flow is symmetric with respect to the origin and hence, we use the fundamental solution $\boldsymbol{S}^{\mathrm{SPP}}$ preserving this symmetry; similarly,

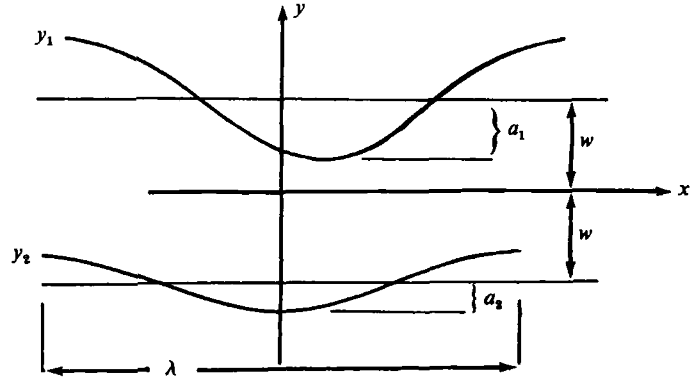

FIGURE 1. Peristaltic flow in a two-dimensional channel with oscillating walls; definition sketch.

for $a_1 = 0$, we use the fundamental solution $\boldsymbol{S}^{\mathrm{WP}}$. For finite values of the mean pressure gradient G, we obtain the flow by an appropriate superposition of the pure peristaltic and the pure pressure driven component, which are calculated independently.

3. Pure peristaltic flow

We begin by considering pure peristaltic flow, $K = 0$, with equal wave amplitudes, $a_1 = a_2 = a$, concentrating on the symmetric case, $\phi = 0$. Asymptotic analysis for small w/λ shows that in narrow channels, the velocity profile over any cross-section is nearly parabolic (Shapiro *et al.* 1969). Onset of trapping is indicated by the appearance of a stagnation point at the channel centreline at the wave frame of reference, occurring approximately when $a/w = 0.60$. This is in excellent agreement with our numerical results. Typical streamline patterns, at both the wave and the stationary frame of reference, are shown in figure 2. In all cases, the velocity profile at the crest and trough of the walls is nearly parabolic in agreement with the asymptotic solution (figure 3*a*).

Let us consider in some detail the size of the development fluid boluses. This information is of physiological and engineering interest, as fluid recirculation owing to onset of boluses may cause thrombosis of blood, or pronounced, undesired, chemical conversion in reactive fluids. We define the bolus height h as the distance between the dividing streamline enclosing the bolus, and the axis of symmetry at $z = 0$, and plot it as a function of wave amplitude (figure 4). There is no bolus for small wave amplitudes but then, as the wave amplitude exceeds the critical value $a/w = 0.60$ the bolus height $h/(w+a)$ increases very fast, and at complete occlusion, $a/w = 1$, it tends to unity. This rapid eddy expansion is reminiscent of that for wall eddies in steady flow as discussed in Pozrikidis (1987, see figure 6). Thus, it indicates that increased sensitivity of viscous eddies with respect to the flow geometry is a general characteristic of creeping motion.

The distribution of shear stress within the fluid is important in applications involving the transport of sensitive materials. High shear stress may cause destruction of blood cells or emulsion drops. To assess the magnitude of shear stress in the flow, we plot the shear stress along the walls (figure 5*a*). Note that since the wall velocity is finite, a change in sign of the shear stress does not imply flow reversal. We observe increased values at the narrow regions of the channel, even for waves

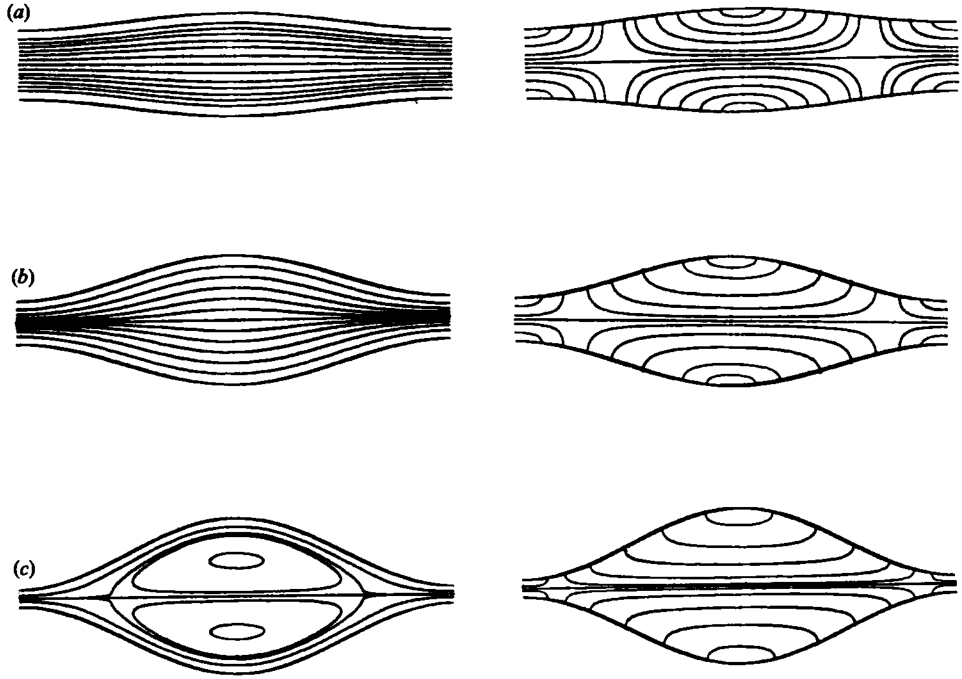

FIGURE 2. Streamline patterns for peristaltic flow in a channel of width $w/\lambda = 0.10$, at the wave (left) and the stationary (right) frame of reference; wave amplitude: (*a*) $a/\lambda = 0.020$, (*b*) $a/\lambda = 0.050$, (*c*) $a/\lambda = 0.080$.

of moderate amplitude, defining limits on wave amplitudes for the transport of sensitive fluids.

Proceeding, we consider flow in wider channels. Our calculations show that the streamline patterns are similar to those for narrow channels, discussed above. However, the velocity profiles significantly deviate from the parabolic shape. As an example, in figure 3(*b*) we present velocity profiles at the trough and crest of the moving wave, for $w/\lambda = 0.50$. It is important to remember that the deviation from the parabolic shape is not due to inertial effects, but to the curvature of the walls. Velocity profiles in a very wide channel are shown in figure 3(*c*), and are in excellent agreement with the asymptotic analysis of Taylor (1951). This analysis is valid for wide channels with small amplitude waves, i.e. large w/λ and small a/λ. Note that the velocity far away from the walls tends to a constant value, equal to $c(ka)^2[1-19(ka)^2/16]/2+O((ka)^6)$. Returning to the $w/\lambda = 0.50$ channel, we note that trapping occurs at a critical wave amplitude, approximately equal to $a/w = 0.50$. The size of the trapped fluid bolus increases rapidly with the wave amplitude as in the narrow channel case (figure 4). The shear stress along the wall exhibits oscillatory behaviour, showing both positive and negative extreme values, figure 5(*b*).

The mean flow rate owing to the peristaltic motion is of particular interest in commercial fluid transport. It is clear that the flow rate vanishes for zero wave amplitude, and becomes maximum at full occlusion, $a/w = 1$. The behaviour for intermediate wave amplitudes depends on both the channel width and wave amplitude, as illustrated in figure 6. For small channel widths, the flow rate increases initially at a parabolic, and then at an almost linear rate with the wave amplitude. This is in agreement with perturbation solutions (Shapiro *et al.* 1969). For large

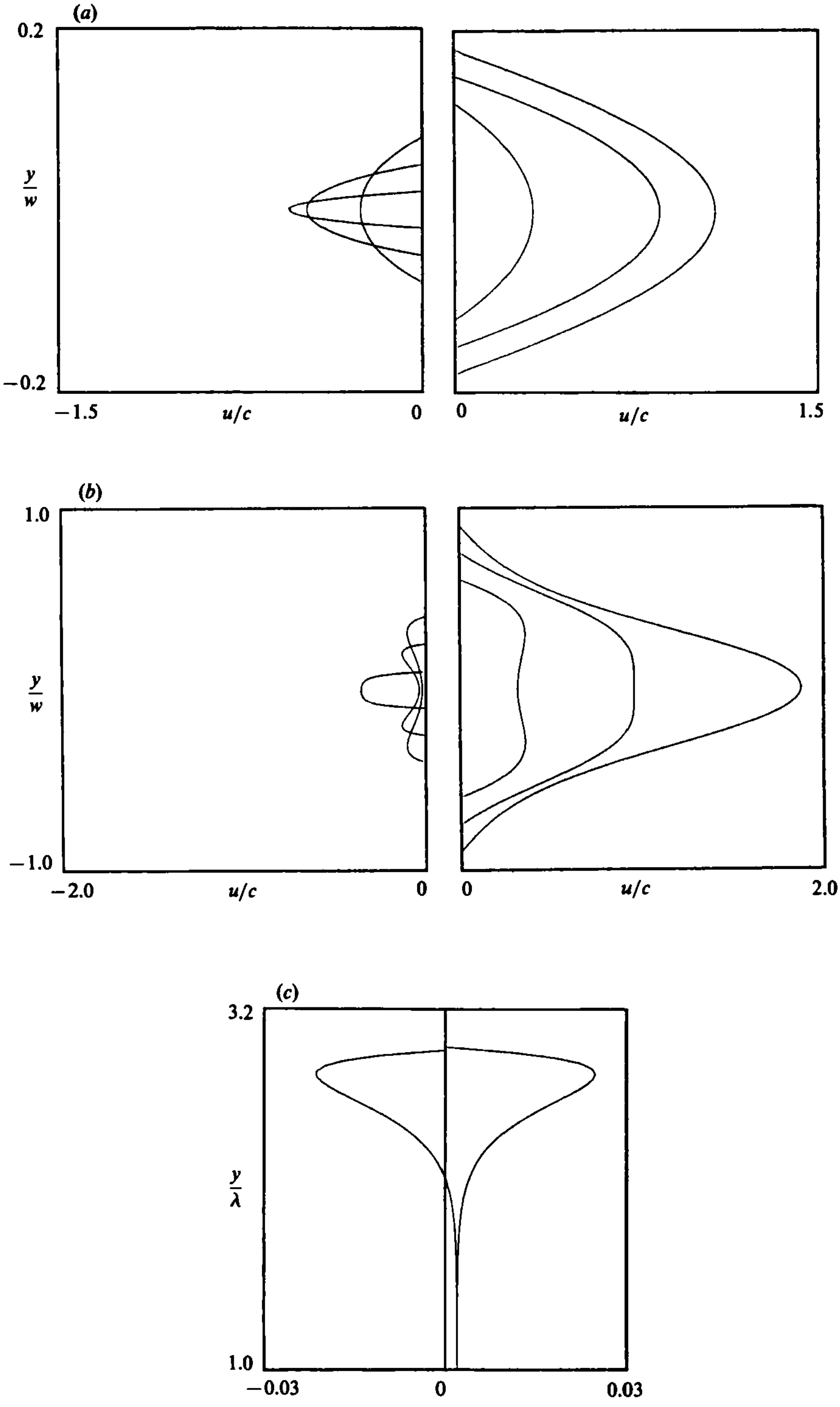

FIGURE 3. Velocity profiles at wave trough (left), and wave crest (right) at the stationary frame, in channels of (*a*) width $w/\lambda = 0.10$, and wave amplitude $a/\lambda = 0.020, 0.050, 0.080$; (*b*) $w/\lambda = 0.50$, and $a/\lambda = 0.100, 0.250, 0.400$; (*c*) $w/\lambda = 3.00$, and $a/\lambda = 0.010$.

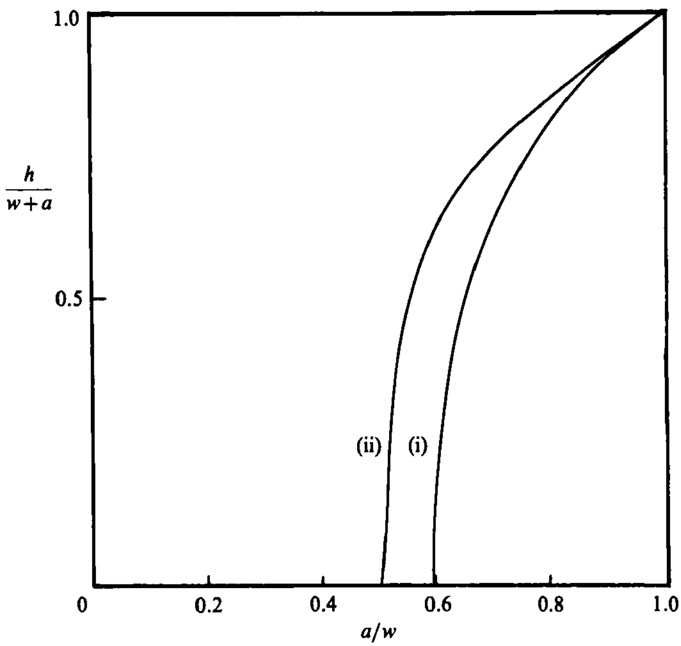

FIGURE 4. Size of free eddies (fluid boluses) at the wave crest as a function of wave amplitude for (i) $w/\lambda = 0.10$, (ii) $w/\lambda = 0.50$.

channel widths, the flow rate increases almost linearly with the wave amplitude. Trapping does not have any apparent effect on the mean flow rate. Overall, our calculations suggest that for a specified wave amplitude to channel width ratio a/w, wide channels provide higher transport rates.

So far we have considered symmetric peristaltic waves with zero phase shift, $\phi = 0$. Now, we wish to investigate the effect of phase shift on the streamline pattern and the mean flow rate. The effect of ϕ on trapping is illustrated in figure 7. Increasing ϕ to $\frac{1}{8}\pi$ causes a rotation and relative displacement of the free eddies around the x-axis. Further increase results in shrinking and disappearance of these eddies. For bending waves, $\phi = \frac{1}{2}\pi$, the streamlines adjust to the curvature of the walls, in a smooth fashion. The effect of phase shift on the mean flow rate $\bar{Q}/cw$ is illustrated in figure 8. For narrow channels, ϕ has a strong effect on the mean flow rate; for the $w/\lambda = 0.10$ channel with wave amplitude $a/\lambda = 0.080$, $\bar{Q}/cw$ is drastically reduced by 98% as ϕ is increased from 0 to $\frac{1}{2}\pi$. Similar behaviour is observed for wider channels, although the dependence of the mean flow rate on the phase shift is less pronounced. For the $w/\lambda = 0.50$ channel with wave amplitude $a/\lambda = 0.30$, the flow rate is moderately reduced by 29% as ϕ is increased from 0 to $\frac{1}{2}\pi$. As the width of the channel w/λ becomes very large, the effect of ϕ on the mean flow rate becomes less important, and vanishes for infinitely wide channels. We conclude that the phase shift may be a significant parameter in the design of peristaltic systems.

4. Effect of mean pressure gradient

In many applications, fluid must be transported against a mean pressure gradient $G = -\mathrm{d}P/\mathrm{d}x$. This significantly alters the flow characteristics with respect to trapping, reflux, and mean flow rate (Shapiro *et al.* 1969).

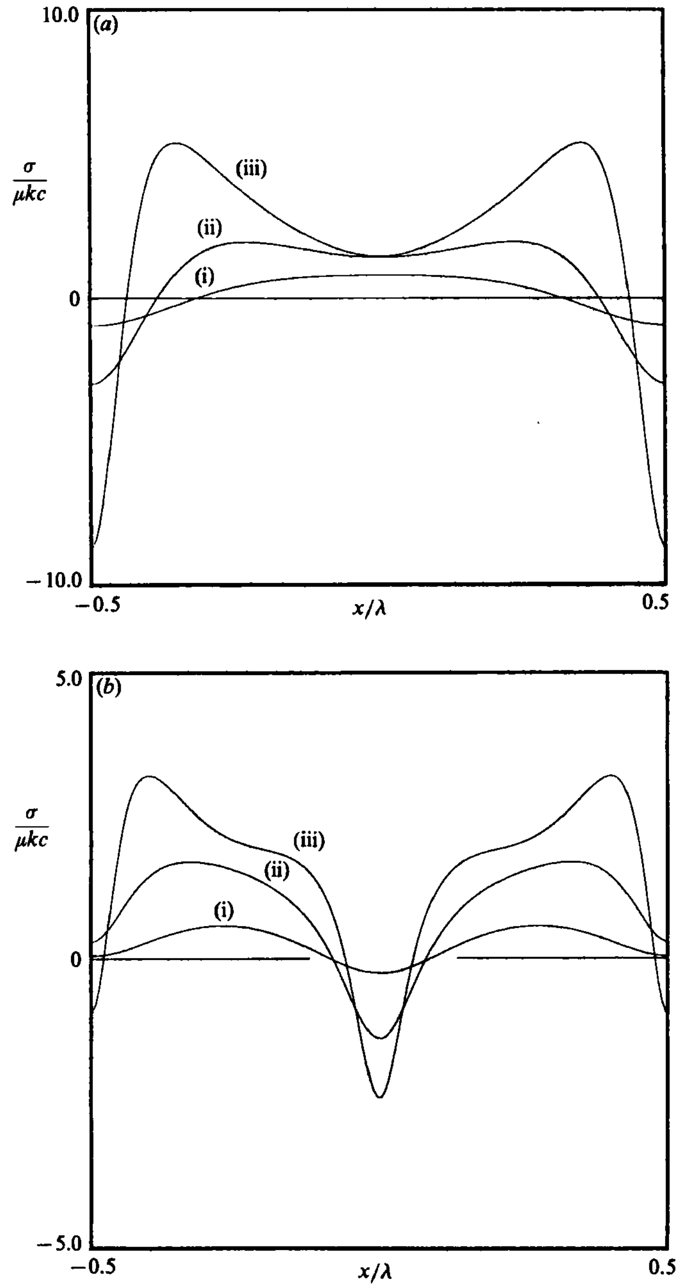

FIGURE 5. Shear stress along the lower wall in a channel of (a) width $w/\lambda = 0.10$ and wave amplitude (i) $a/\lambda = 0.020$, (ii) $a/\lambda = 0.050$, (iii) $a/\lambda = 0.080$; (b) $w/\lambda = 0.50$, and (i) $a/\lambda = 0.100$, (ii) $a/\lambda = 0.250$, (iii) $a/\lambda = 0.400$.

First, we consider the effect of mean pressure gradient on trapping. Shapiro *et al.* (1969) showed that for narrow channels, increasing the opposing pressure gradient causes a reduction in the bolus size and eventually, collapse of the bolus into a stagnation point along the channel centreline, at $z = 0$. Thus, they suggested that onset of trapping is indicated by appearance of a stagnation point on the z-axis. This

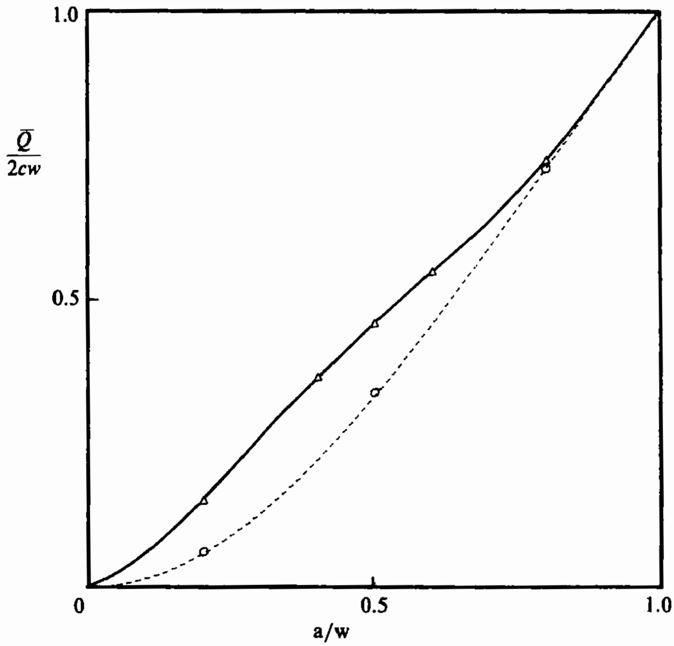

FIGURE 6. Mean flow rate as a function of wave amplitude for peristaltic flow in a channel of (i) ○, $w/\lambda = 0.10$, (ii) △, $w/\lambda = 0.50$; the dashed lines shows results of asymptotic theory for small w/λ (Shapiro *et al.* 1969).

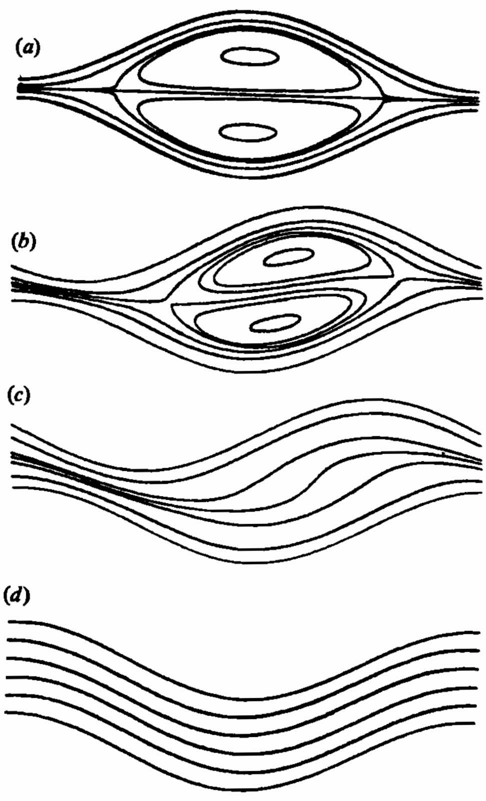

FIGURE 7. Streamline patterns for flow in a channel with $w/\lambda = 0.10$, $a/\lambda = 0.080$, at the wave frame of reference; phase shift: (*a*) $\phi = 0$, (*b*) $\phi = \frac{1}{8}\pi$, (*c*) $\phi = \frac{1}{4}\pi$, (d) $\phi = \frac{1}{2}\pi$.

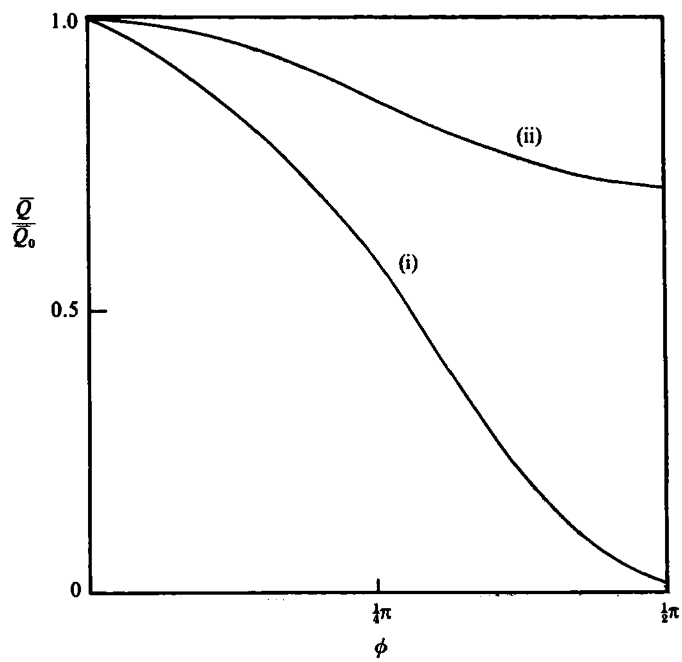

FIGURE 8. Effect of phase shift ϕ on the mean flow rate for (i) $w/\lambda = 0.100$, $a/\lambda = 0.080$, (ii) $w/\lambda = 0.500$, $a/\lambda = 0.300$; Q_0 is the mean flow rate at $\phi = 0$.

criterion was used by other investigators to resolve trapping in wider channels. To examine the validity of this criterion, we consider flow in a channel of $w/\lambda = 0.50$ with $a/\lambda = 0.300$, $\phi = 0$, for different values of the mean pressure ratio $K = Gw^2/\mu c$ (figure 9). As the opposing pressure field is increased, the size of the free eddies decreases, and at a critical point, the eddies detach, leaving a narrow passage at the channel centreline (figure 9*b*, *c*). Further increase in the opposing pressure field results in elimination of the free eddies. This shows that trapping is not necessarily associated with a stagnation point at the channel centreline. It is determined by the complex interaction between the peristaltic and the pressure-driven motion.

Shapiro *et al.* (1969) showed that the presence of an opposing mean pressure gradient may cause the net upstream transport of fluid particles, i.e. material reflux. To establish criteria for reflux, they noticed that the motion of a fluid particle is periodic. The period T of a particle outside a trapped bolus is equal to the time required for the particle to travel a distance equal to one wavelength λ along the z-axis; fluid particles lying on the same streamline have identical periods of motion. Our calculations show that during its evolution, a material line initially coinciding with an open streamline retains an almost sinusoidal shape, suffering compression and elongation at either end. The paths of the individual material particles constitute spiral lines, in agreement with previous studies. The x-distance travelled by these particles during one period is equal to $Tc-\lambda$. This defines a mean convection speed $u_c = (Tc-\lambda)/T$, with a negative value implying reflux. Our calculations show that for small channel widths (increasing the opposing pressure gradient), reflux first occurs for particles near the walls of the channel and then it extends towards the centre of the channel. This is in agreement with the asymptotic analysis of Shapiro *et al.* (1969). On the other hand, for large channel widths, reflux may first occur at

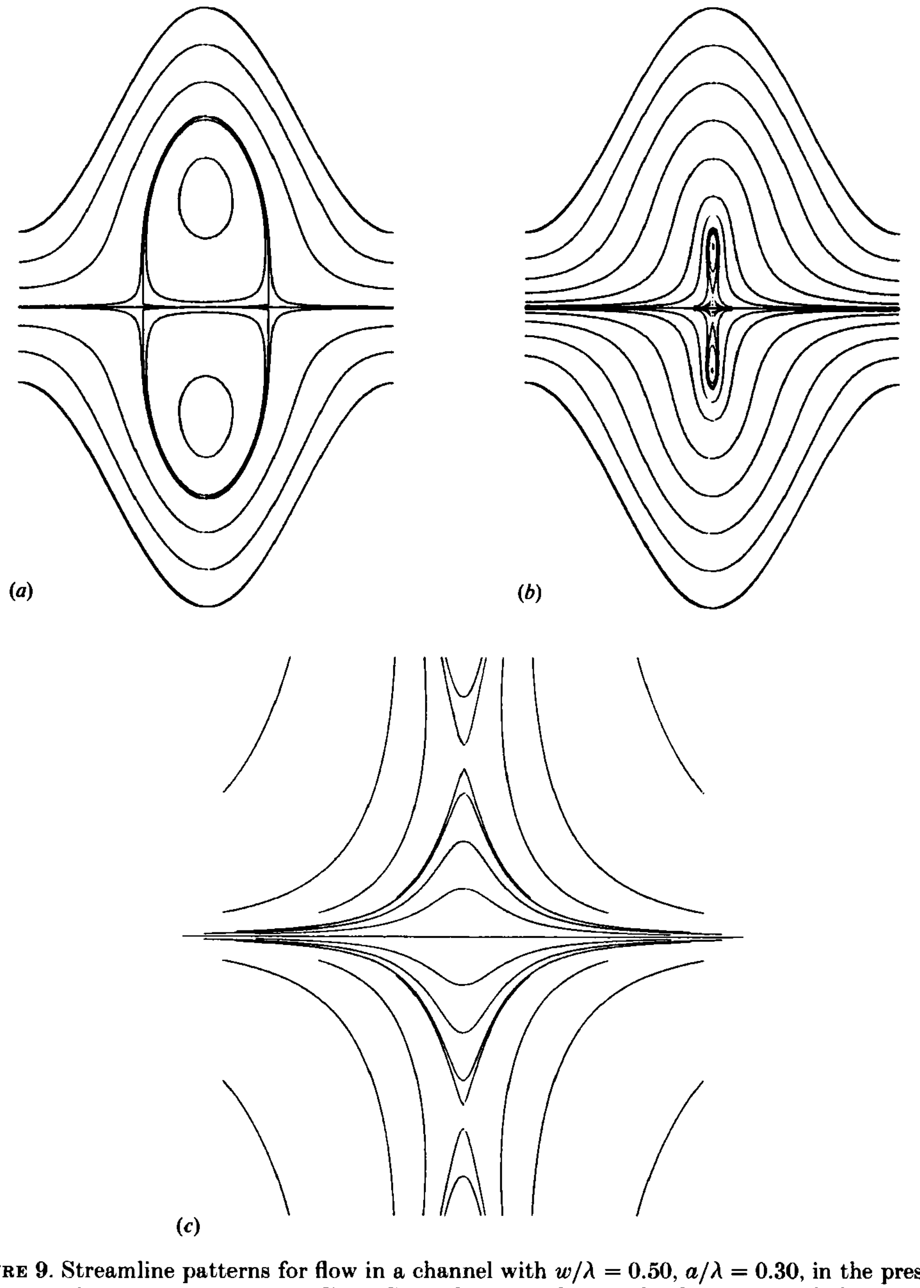

FIGURE 9. Streamline patterns for flow in a channel with $w/\lambda = 0.50$, $a/\lambda = 0.30$, in the presence of an opposing mean pressure gradient G, at the wave frame of reference; (a) $Gw^2/\mu c = 0$, (b) $Gw^2/\mu c = -0.4615$, (c) detail of central region of (b).

the channel centreline. This behaviour is illustrated in figure 10, where we plot the distribution of mean convection speed u_c/c along the vertical line through the origin, for two characteristic cases. The observed variation indicates the complexity of Lagrangian dynamics in peristaltic systems.

It is interesting to consider the flow due to a strong pressure gradient in the presence of weak peristaltic motion. This is relevant to the locomotion of microscopic

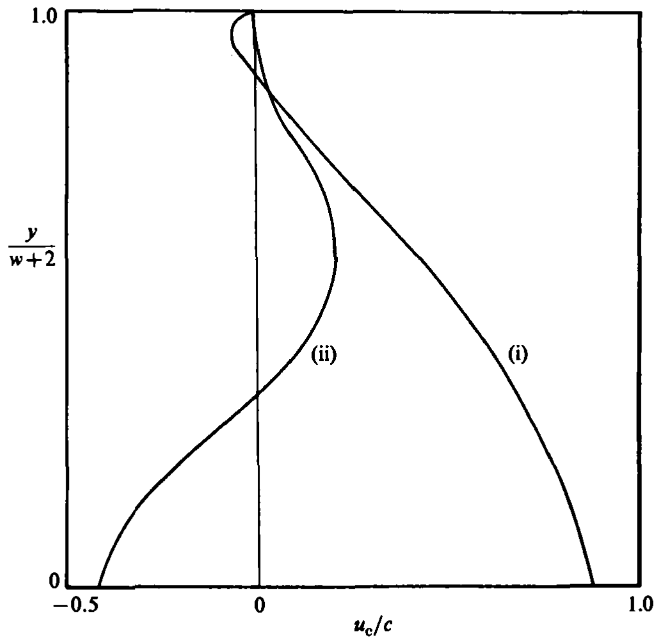

FIGURE 10. Mean particle convection velocity u_c/c along the vertical line at $x = 0$, for (i) $w/\lambda = 0.10$, $a/\lambda = 0.080$, $Gw^2/\mu c = 20.222$, (ii) $w/\lambda = 0.50$, $a/\lambda = 0.300$, $Gw^2/\mu c = 10.00$.

organisms in external flow. First, let us consider the limiting flow as the peristaltic motion ceases, i.e. $K \rightarrow \infty$. In this limit, the flow reduces a pure pressure-driven flow in a symmetric channel with sinusoidal walls. Our previous analysis (Pozrikidis 1987 §4) indicates that for large channel widths and wave amplitudes, the flow will reverse at the trough of the corrugations, forming wall eddies. A typical streamline pattern for $w/\lambda = 0.50$ and $a/\lambda = 0.300$ is presented in figure 11(*a*). Now, when a weak peristaltic component is introduced, the eddies must detach from the walls, merely from kinematical principles. The resulting flow pattern depends on the direction of wave propagation. When the mean pressure field opposes the peristaltic motion, $K < 0$, an asymmetric pair of eddies develops (figure 11*b*, *c*). When the mean pressure field and the peristaltic motion act in the same direction, $K < 0$, the eddies expand, approach the channel centreline, and give rise to trapping (figure 11*d*).

The above results are valid for steady flow conditions. However, under the quasi-steady approximation, they may be extended for slowly varying flow conditions, i.e. low Strouhal numbers (Sobey 1980). An interesting interpretation arises from this observation. Consider peristaltic flow in a wide channel with large amplitude waves, and in the presence of a slowly varying mean pressure gradient. When the pressure component dominates, the flow will tend to separate at the trough of the wavy wall. When the peristaltic component dominates, the flow will tend to separate along the channel centreline. This oscillatory behaviour will enhance the fluid mixing, and thus, will increase the efficiency of simultaneous molecular–convective processes (Sobey 1980). In conclusion, it suggests an efficient engineering process for heat or mass transfer.

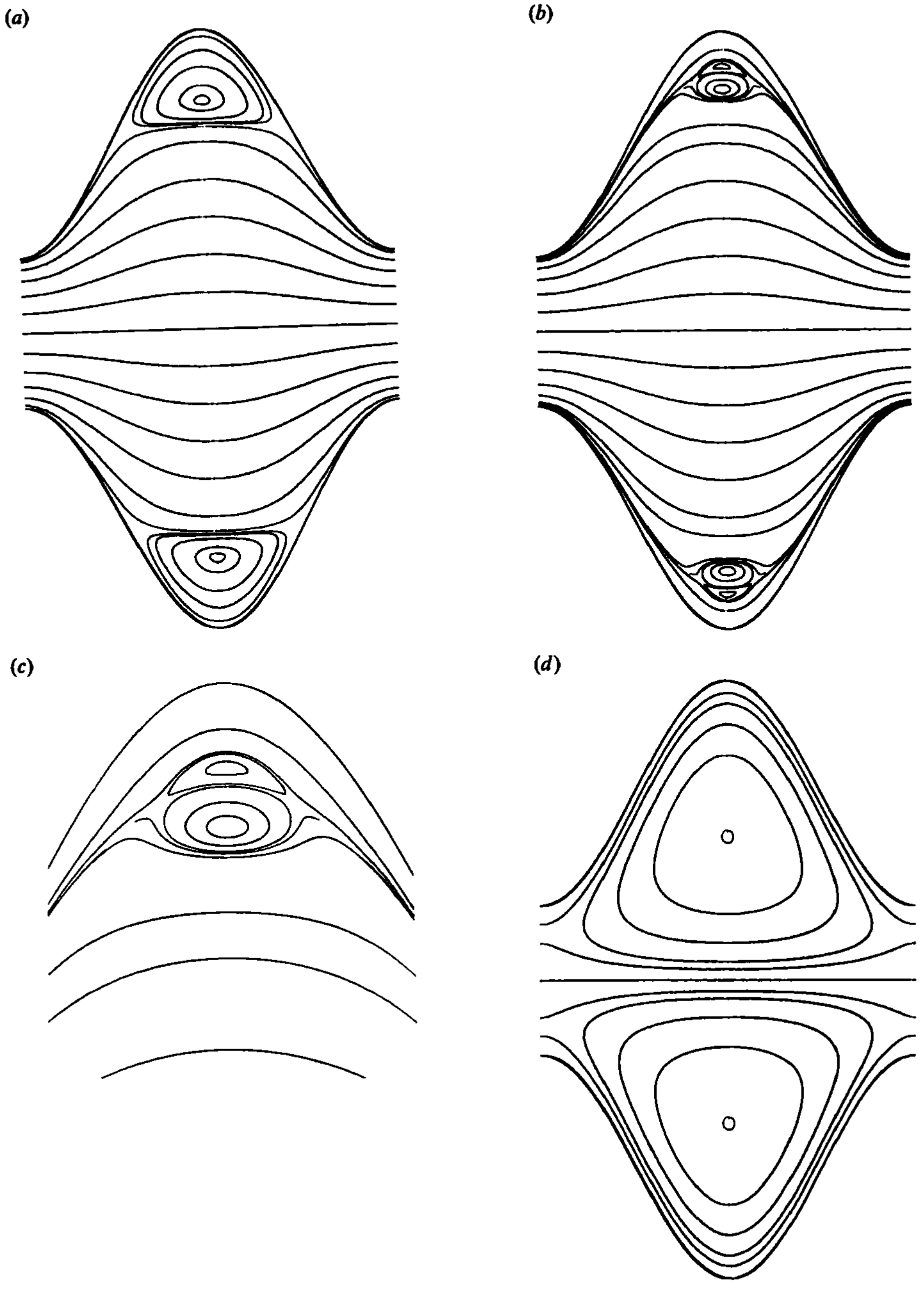

FIGURE 11. Effect of peristaltic motion on the streamline pattern for pressure driven flow in a channel of $w/\lambda = 0.50$, $a/\lambda = 0.30$; (a) $\mu c/Gw^2 = 0$, (b) $\mu c/Gw^2 = -0.0005005$, (c) detail of (b), (d) $\mu c/Gw^2 = 0.010204$.

5. Asymmetric waves

In our previous discussion we considered waves of equal amplitude $a_1 = a_2 = a$. These represent specific configurations, convenient for the mathematical analysis. In practice, it may be necessary to use waves of different amplitudes. We consider how these waves affect the flow characteristics.

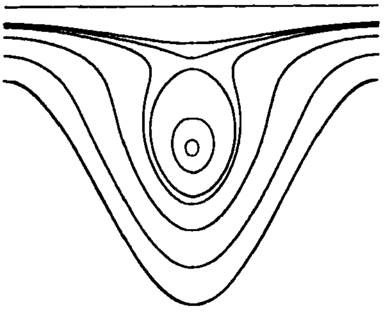

FIGURE 12. Streamline pattern for asymmetric flow in a channel with $w/\lambda = 0.50$, $a_2/\lambda = 0.300$, $a_1/\lambda = 0$, at the wave frame of reference.

Our calculations show that asymmetric waves do not alter the basic features of the motion discussed previously, in agreement with the asymptotic analysis of Yin & Fung (1971). An example with asymmetric waves of $w/\lambda = 0.50$, $a_2/\lambda = 0.300$, $a_1/\lambda = 0$ is shown in figure 12. We note the presence of a single fluid bolus translating at the wave speed, i.e. trapping.

I would like to thank Professor J. J. L. Higdon for suggesting the present work. The support of Eastman Kodak company is acknowledged.

REFERENCES

BOHME, G. & FRIEDRICH, R. 1983 Peristaltic flow of viscoelastic liquids. *J. Fluid Mech.* **128**, 109–122.

BROWN, T. D. & HUNG, T. K. 1977 Computational and experimental investigation of two-dimensional nonlinear peristaltic flows. *J. Fluid Mech.* **83**, 249–272.

HUNG, T. K. & BROWN, T. D. 1976 Solid-particle motion in two-dimensional peristaltic flows. *J. Fluid Mech.* **73**, 77–96.

JAFFRIN, M. Y. & SHAPIRO, A. H. 1971 Peristaltic pumping. *Ann. Rev. Fluid Mech.* **3**, 13–36.

LYKOODIS, P. S. & ROOS, R. 1970 The fluid mechanics of the ureter from a lubrication point of view. *J. Fluid Mech.* **43**, 661–674.

POZRIKIDIS, C. 1987 Creeping flow in two-dimensional channels. *J. Fluid Mech.* **180**, 495–514.

SHAPIRO, A. H., JAFFRIN, M. Y., WEINBERG, S. L. 1969 Peristaltic pumping with long wavelengths at low Reynolds numbers. *J. Fluid Mech.* **37**, 799–825.

SHUKLA, J. B., PARIHAR, R. S. & RAO, B. R. 1980 Effects of peripheral-layer viscosity on peristaltic transport of a bio-fluid. *J. Fluid Mech.* **97**, 225–237.

SOBEY, I. J. 1980 On flow through furrowed channels. Part 1. Calculated flow patterns. *J. Fluid Mech.* **96**, 1–26.

TAKABATAKE, S. & AYUKAWA, K. 1982 Numerical study of two-dimensional peristaltic flows. *J. Fluid Mech.* **122**, 439–465.

TAYLOR, G. I. 1951 Analysis of the swimming of microscopic organisms. *Proc. R. Soc.* A **209**, 447–461.

TONG, P. & VAWTER, D. 1972 An analysis of peristaltic pumping. *J. Appl. Maths* **33**, 857–869.

WILSON, D. E. & PANTON, R. L. 1979 Peristaltic transport due to finite amplitude bending and constructing waves. *J. Fluid Mech.* **90**, 145–159.

YIN, F. C. P. & FUNG, Y. C. 1971 Comparison of theory and experiment in peristaltic transport. *J. Fluid Mech.* **47**, 93–112.